IEEE Access
Multidisciplinary ⋮ Rapid Review ⋮ Open Access Journal

Received May 15, 2021, accepted May 24, 2021, date of publication June 4, 2021, date of current version June 15, 2021.

Digital Object Identifier 10.1109/ACCESS.2021.3086232

A Belief Coulomb Force in D-S Evidence Theory

BO FU[1], JINWEI FANG[1], XILIN ZHAO[1], XING CHEN[2], KANG XU[1], AND ZHANGQING HE[1]
[1]School of Electrical and Electronic Engineering, Hubei University of Technology, Wuhan 430072, China
[2]School of Mechanical and Electrical Engineering, University of Southern Queensland, Toowoomba, QLD 4350, Australia

Corresponding authors: Bo Fu (xiaoxing.zhang@outlook.com), JinWei Fang (1007053916@qq.com), and Xilin Zhao(zhaoxl@mail.hbut.edu.cn)

This work was supported by the Natural Science Foundation of the Provincial Science and Technology Department under Grant 2020CFB814.

ABSTRACT Dempster-Shafer (D-S) evidence theory is regarded as an effective method of dealing with the uncertainty of the information but still suffers from the conflict problem among the evidence. Despite that various techniques were presented in plenty of publications, currently, there is no convincing evidence and firm conclusion about the optimum solution. This study presents Belief Coulomb Force (BCF) into D-S evidence theory, where Zhou *et al.* entropy is applied to represent the electrical charge of the belief function, and the Coulomb gravity or repulsion would be identified with the Pearson correlation coefficient. According to the simulation results, the recognition accuracy on malfunction diagnosis of the presented approach reaches 93.7%, and the effectiveness of analyzing the conflict evidence problem can be demonstrated from the comparison with the previous methods.

INDEX TERMS Belief Coulomb force, Pearson correlation coefficient, D-S evidence theory, fault diagnosis, information fusion.

I. INTRODUCTION

Once firstly introduced by Dempster [1], D-S evidence theory was further improved by Shafer [2]. Due to its superiority on manipulating the uncertain information, it was diversely applied into machine learning [3], like rough set [6], [7], fuzzy set [4], [5], Z value [8], [9], D number [11], [12], belief structure [10], soft likelihood function (SLF) [13], confidence function [18] and belief entropy [16], [17]. As a powerful tool for analyzing the fusion and expression of decision-level uncertainty information, D-S evidence theory appears to offer sufficiently broad applicability in fault diagnosis [9], [21], decision analysis [22], [23], and information fusion [19], [20]. Particularly, the evidence information fusion from multiple independent sources is mainly performed with Dempster's combination rule. Nevertheless, a counterexample was found by Zadeh [24] that once the contradictory evidence combines, the results would not be ideal as we expected. And much attention has been paid to this issue in the conflicting studies.

To date, two main ideas were put forward for solving the conflict problem. The first one is to improve the classic D-S evidence theory's combination rules to adapt to a highly conflicting environment, that is, to modify the combination rules to redistribute conflicts. Lefevre *et al.* [25] proposed the "unified reliability function combination method" to modify the combination rule. Several methods include Yager [26], [27], Inagaki [28], and so on, were proposed under this kind of idea. They introduced the method of average support for the proposition. Fixsen and Mahler [29], Daniel [30] proposed the *minC* combination rules with refining the allocation space and local conflict and potential conflict. Ma *et al.* [32] recently proposed a set of flexible combination rules from the entire conflict set. F. Xiao proposed a generalized Dempster-Shafer (D-S) combination rule [31]. Compared with the classic Dempster combination rule, the generalized Dempster-Shafer combination rule is more general and applicable. The second class is to preprocess the conflicting evidence before fusion by retaining the classical evidence theory's combination rules [33]. Typical methods include the weighted average Deng method [35], [37] and Murphy's simple arithmetic average method [34]. Currently, Haenni's view is most widely supported by the researchers to modify the data model. Particularly, by considering the applicability of the Dempster merger rule in various conflict situations, Xiao [36] presented a new method to enhance the measure of belief divergence. The correlations between belief functions and subsets of the sets of belief functions are considered for the first time. Jing and Tang [14] proposed a new base basic probability

The associate editor coordinating the review of this manuscript and approving it for publication was M. Venkateshkumar.

assignment (bBPA) method to deal with potential conflicts before data fusion. Yongchuan Tang *et al.* [15] considered the modeling of uncertain information from the closed-world to the open-world hypothesis and studied the generation of basic probability assignments with incomplete information. Liu [38] described the conflicts with the two-tuple of k and difBetP. Xiao *et al.* [50] introduced a novel coefficient as the measurement on the correlation between two pieces of evidence.

As introduced above, the whole research is based upon Coulomb force theory, the background therefore would be explained. Coulomb's law was first proposed by Charles Augustin de Coulomb in The Law of Electricity in 1785. Coulomb's law interprets the interaction force between two static charges in a vacuum, which is proportional to the product of their electrical charge whereas inversely proportional to the square of their distance. The direction of the force is on their connection line. The same kind of charges would repel each other whereas the different kinds of charges attract each other. Thus, Lee and Park [39] simulated eddy currents within the integrated physical model based on the idea of Coulomb's law, and lots of concerns were received. Subsequently, an increasing number of scholars have applied novel algorithms combining physical meaning to relevant scientific research fields [40], [41], [49].

In this paper, the belief Coulomb Force (BCF) in D-S evidence theory was creatively proposed. We believed that the essence of evidence information fusion would be affected by some potential force, which could be attractive or repulsive. At the existence of the attraction force, the evidence would be merged. Whereas they cannot be merged when there is repulsion force. Moreover, the degree of these forces between the evidence can be quantified by the presented BCF.

The main contributions in this article can be summarized as follows:

- This is the first time when electromagnetic theory has been introduced into evidence theory;
- Using the belief Coulomb force to measure the degree of conflict between evidence;
- Applying the Pearson correlation coefficient to judge under what conditions the evidence can be fused. When the Pearson correlation coefficient is greater than 0, there is Coulomb gravitation between the evidence and the evidence can be fused, and vice versa.

The content of this paper can be divided into multiple parts as follows. The relevant knowledge needed for understanding is introduced in section 2. Then, section 3 puts forward the BCF theory and formula and demonstrates the basic properties. In section 4, a numerical example simulates and displayed the process of information fusion in evidence theory. The nature of the method is illustrated in the next section. Additionally, the conflict measurement is conducted with the proposed BCF formula in section 6 and the performance is evaluated according to the comparison. The final 2 sections demonstrate its promising application in fault diagnosis and summarize the work of this article.

II. PREPARATION

Here, we would review several basic ideas on D-S evidence theory, Jiang conflict coefficient, Pearson correlation coefficient, and Coulomb's law.

A. D-S EVIDENCE THEORY

1) IDENTIFICATION FRAMEWORK

Definition 1: Let $\Theta = \{\theta_1, \theta_2, \ldots, \theta_n\}$, which is called the recognition framework, denote a set of mutually exclusive finite groups. The 2^Θ is the Θ power set and contains all the propositions, which can be defined as follows

$$2^\Theta = \{\phi, \{\theta_1\}, \ldots, \{\theta_n\}, \{\theta_1, \theta_2\}, \ldots, \{\theta_1, \theta_2, \ldots \theta_i\}, \ldots, \Theta\}, \tag{1}$$

where the empty set is represented by ϕ. If $A \in 2^\Theta$ then A could be named as a proposition.

2) MASS FUNCTION

Definition 2: As for the recognition framework Θ, the mass function, mapping m from 2^Θ to [0,1], is represented as

$$m : 2^\Theta \to [0, 1], \tag{2}$$

which meets the following two attributes

$$m(\emptyset) = 0 \; and \; \sum_{\theta \subseteq \Theta} m(A) = 1. \tag{3}$$

In (3), $m(A)$ is the Basic Probability Assignment (BPA) of proposition A, which stands for the degree to which A is supported. When $m(A) > 0$, A can be viewed as the focal element of the mass function.

3) DEMPSTER'S COMBINATION RUL

Definition 3: Assuming that $m_i(i=1,2,\ldots,5)$ stands for the i-th evidence for the whole article. Meanwhile, m_1 and m_2 are defined in the recognition framework, the definition of Dempster's combination rule can be shown as follows ($\oplus$ means the orthogonal sum operation.)

$$[m_1 \oplus m_2](\theta) = \begin{cases} \dfrac{\sum_{A_1 \cap A_2 = \theta} m_1(A_1) \cdot m_2(A_2)}{1-k} & \theta \neq \emptyset \\ 0 & \theta = \emptyset. \end{cases} \tag{4}$$

where the parameter k [1], conflict coefficient, can be represented as

$$k = \sum_{A_1 \cap A_2 = \emptyset} m_1(A_1) \cdot m_2(A_2). \tag{5}$$

This rule would valid when $k < 1$.

B. THE JIANG CONFLICT COEFFICIENT

Jiang [44] proposed a new kind of coefficient to describe the conflict evidence.

Definition 4: In a recognition frame Θ within N elements, it can be assumed that the mass functions of the two pieces of evidence represented by m_1 and m_2, the Jiang conflict coefficient is defined as

$$k_r(m_1, m_2) = 1 - \frac{c(m_1, m_2)}{\sqrt{c(m_1, m_1) \cdot c(m_2, m_2)}}, \tag{6}$$

where $c(m_1, m_2)$ measures the correlation

$$c(m_1, m_2) = \sum_{i=1}^{2^N} \sum_{j=1}^{2^N} m_1(A_i) m_1(A_j) \left| \frac{A_i \cap A_j}{A_i \cup A_j} \right|, \tag{7}$$

where $i, j = 1, \ldots, 2^N$, A_i and A_j are the focus elements of mass function, |. | represents the cardinality of the subset.

The Jang conflict coefficient $k_r(m_1, m_2)$, whose value range is [0,1], is the conflict measurement between m_1 and m_2. The greater Jiang conflict coefficient is thought to reflect the greater conflict between m_1 and m_2. $k_r = 1$ means a complete contradiction between m_1 and m_2. Otherwise, $k_r = 0$ means no conflict between m_1 and m_2.

C. PEARSON CORRELATION COEFFICIENT (PCC)

PCC [45], proposed by Pearson firstly, is used to measure the correlation between two variables. The definition is shown below

Definition 5: For the same assumption made in *Definition 4*, PCC can be defined as

$$\begin{aligned} &\rho(m_1, m_2) \\ &= \frac{COV(m_1, m_2)}{\sigma_{m_1}\sigma_{m_2}} = \frac{E[(m_1 - \mu_{m_1})(m_1 - \mu_{m_2})]}{\sigma_{m_1}\sigma_{m_2}} \\ &= \frac{\sum_{i=1}^{2^N} \left(m_1(A_i) - \mu_{m_1}\right) \cdot \left(m_2(B_i) - \mu_{m_2}\right)}{\sqrt{\left[\sum_{i=1}^{2^N} \left(m_1(A_i) - \mu_{m_1}\right)^2\right] \cdot \left[\sum_{i=1}^{2^N} \left(m_2(B_i) - \mu_{m_2}\right)^2\right]}}, \end{aligned} \tag{8}$$

where $i = 1, \ldots 2^N$, $COV(m_1, m_2)$, σ_{m1}, σ_{m2}, $m_1(A_i)$, μ_{m1}, $m_2(B_i)$, and μ_{m2} are the covariance between $m_1(\bullet)$ and $m_2(\bullet)$, the standard deviation of $m_1(\bullet)$, the standard deviation of $m_2(\bullet)$, the BPA of proposition A_i in $m_1(\bullet)$, the average probability vector of all propositions in $m_1(\bullet)$, the BPA of proposition B_i in $m_2(\bullet)$, and the average probability vector of all propositions in $m_2(\bullet)$ respectively.

$\rho(m_1, m_2) \in [-1,1]$ measures the correlation between $m_1(\bullet)$ and $m_2(\bullet)$. When $\rho > 0$ (or $\rho < 0$), a positive (or negative) correlation can be indicated. Whereas there is no correlation when $\rho = 0$.

D. COULOMB'S LAW

Definition 6: Let F be the magnitude of Coulomb force on the object, K_e be the Coulomb constant, Q_1 and Q_2 be the magnitude of two charges, and R be the distance between the two charges. Then, the defined Coulomb force formula is shown as

$$F = K_e \frac{Q_1 Q_2}{R^2}. \tag{9}$$

In Eq.(9), the law can be expressed as the condition when the gravitation or repulsion appears between any two charges in a vacuum. The magnitude of the Coulomb force positively correlates with the electrical charges and is inversely associated with the square of their distance.

III. THE THEORY OF BELIEF COULOMB FORCE

Motivated by the Coulomb force theory, we propose a novel BCF basing upon evidence theory.

A. ELECTRICAL CHARGE BASED ON ZHOU et al. ENTROPY

Deng entropy [42] is a commonly used belief entropy to quantify uncertainty information, but it only focuses on the mass function itself and ignores the available information represented by the scale of the identification frame in the evidence subject [43]. However, Zhou *et al.* entropy [43] considered the scale of the recognition frame and the relative scale of a focal element with reference relative to this frame, and the information described is more comprehensive.

Definition 7: Assuming that mass function m is in the recognition framework, the Zhou *et al.* entropy formula is expressed as

$$Q_m = -\sum_{A \subseteq \Theta} m(A) log_2 \left(\frac{m(A)}{2^{|A|} - 1} e^{\frac{|A|-1}{|\Theta|}} \right), \tag{10}$$

where A is a proposition in the mass function m, $|A|$ is the cardinality of A, Θ is the recognition frame, Θ is the cardinality of the recognition frame, and $2^{|A|} - 1$ is the number of potential states in A.

Assumption 1: Assume that m_1 and m_2 defined in the same recognition framework $\Theta = \{A_1, A_2, A_3\}$, where A_1, A_2, *and* $A_3 \notin \varnothing$, and their BPA is as follows

$m_1 : m_1(A_1) = V_1, m1(A_2) = V_2, m_1(A_3) = V_3$ and $m_2 : m_2(A_1) = S_1, m_2(A_2) = S_2, m_2(A_3) = S_3$.

Calculation: Based on (10), the electrical charge of the evidence m_1 is

$$\begin{aligned} Q_{m_1} = &-\left[V_1 \times log_2 \left(\frac{V_1}{2^{|1|} - 1} \times e^{\frac{|1|-1}{|3|}} \right) + V_2 \right. \\ &\left. \times log_2 \left(\frac{V_2}{2^{|1|} - 1} \times e^{\frac{|1|-1}{|3|}} \right) + V_3 \times log_2 \left(\frac{V_3}{2^{|1|} - 1} \times e^{\frac{|1|-1}{|3|}} \right) \right] \\ = &-(\mathrm{V}_1 \times \log_2 \mathrm{V}_1 + \mathrm{V}_2 \times \log_2 \mathrm{V}_2 + \mathrm{V}_3 \times \log_2 \mathrm{V}_3). \end{aligned}$$

Similarly, the electrical charge of the evidence m_2 is

$$\begin{aligned} Q_{m_2} = &-\left[S_1 \times log_2 \left(\frac{S_1}{2^{|1|} - 1} \times e^{\frac{|1|-1}{|3|}} \right) + S_2 \right. \\ &\left. \times log_2 \left(\frac{S_2}{2^{|1|} - 1} \times e^{\frac{|1|-1}{|3|}} \right) + S_3 \times log_2 \left(\frac{S_3}{2^{|1|} - 1} \times e^{\frac{|1|-1}{|3|}} \right) \right] \\ = &-(\mathrm{S}_1 \times \log_2 \mathrm{S}_1 + \mathrm{S}_2 \times \log_2 \mathrm{S}_2 + \mathrm{S}_3 \times \log_2 \mathrm{S}_3). \end{aligned}$$

B. THE DISTANCE OF COULOMB EVIDENCE

By considering the differences between focus and non-focus elements, the Jiang conflict coefficient [48] can measure the inconsistency effectively and satisfy many desirable properties, which might be promising in the study with regard to similarity or relevance measurement. Hence, the Coulomb evidence distance was constructed by the Jiang conflict coefficient.

Definition 8: As defined in *Definition 4 and 5*, the Coulomb evidence distance between m_1 and m_2 is shown below

$$d\left(m_1, m_2\right)=\sqrt{k_r\left(m_1, m_2\right)}=\sqrt{1-\frac{c\left(m_1, m_2\right)}{\sqrt{c\left(m_1, m_1\right)\cdot c\left(m_2, m_2\right)}}}. \tag{11}$$

The properties of Coulomb evidence distance can be summarized as follows:

Non-negativity: $d(m_1, m_2) \geq 0$, when $m_1 \neq m_2$, $d(m_1, m_2) > 0$.

Non-degeneracy: $d(m_1, m_2) = 0 \leftrightarrow m_1 = m_2$.

Symmetry: $d(m_1, m_2) = d(m_2, m_1)$.

Triangular inequality: $d(m_1, m_2) \leq d(m_1, m_3)+ d(m_3, m_2)$, for any m_3 in the same recognition frame.

C. THE BELIEF COULOMB FORCE FORMULA AND PERFORM MODEL ANALYSIS

In this subsection, we propose a novel BCF formula derived from the electrical charge of evidence and the Coulomb evidence distance.

1) THE BELIEF COULOMB FORCE FORMULA

Definition 9: As assumed above, the BCF formula based upon (9) can be defined as

$$F_{BCF} = K_{ET}\frac{Q_{m1}Q_{m2}}{d^2}, \tag{12}$$

where K_{ET} is

$$K_{ET} = 2^{-\varepsilon|\Theta|} \tag{13}$$

with

$$0 \leq \varepsilon \leq 1. \tag{14}$$

In Eq. (12), Q_{m1} and Q_{m2} are the electrical charges of m_1 and m_2 respectively. $d(m_1, m_2)$ is the Coulomb evidence distance between them. K_{ET} is the Coulomb force parameter, which is applied to differentiate the discernment frames. ε stands for a flexible variable of (13) and the size of the BCF can be dynamically regulated for more clear observation. Simultaneously, ε value in different BCF formulas must be consistent for a determinate system.

2) MODEL ANALYSIS

The BCF formula model is shown in Fig. 1.

Assumption 2: Assuming that m_1, m_2, and m_3 are three pieces of evidence defined in the same recognition framework $\Theta = \{A_1, A_2, A_3\}$, their BPA is as follows:

$m_1 : m_1(A_1)=0.99,\ m_1(A_2)=0.01,\ m_1(A_3)=0$

$m_2 : m_2(A_1)=0.97,\ m_2(A_2)=0.03,\ m_2(A_3)=0$

$m_3 : m_3(A_1)=0,\ m_3(A_2)=0.01,\ m_3(A_3)=0.99.$

Physical significance $F_{BCF}(m_i, m_j)$ denotes the Coulomb force between m_i and m_j. $\rho(m_i, m_j)$ is PCC between m_i and m_j. Because PCC [45] is the measurement of the correlation, we believe that the stronger the correlation is, the stronger the force would be. When PCC is greater than 0, there is Coulomb

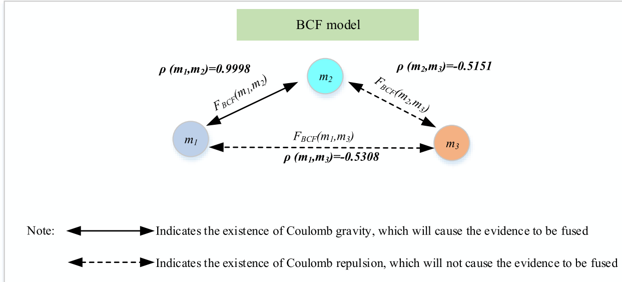

FIGURE 1. **Principle model diagram of BCF.**

gravitation between m_i and m_j. If PCC is 1, the Coulomb gravitation reaches the maximum value. When PCC is less than 0, there is Coulomb repulsion between m_i and m_j. If PCC is -1, the Coulomb repulsion reaches the maximum value.

Analysis In Fig. 1, since $\rho(m_1, m_2) > 0$, there is Coulomb gravitational force between m_1 and m_2, whose magnitude can be represented by $F_{BCF}(m_1, m_2)$, m_1 and m_2 can be fused. Because of $\rho(m_2, m_3) < 0$, there is Coulomb repulsion between m_2 and m_3. $F_{BCF}(m_2, m_3)$ represents the size of the Coulomb repulsion, so m_2 and m_3 cannot be fused. Due to $\rho(m_1, m_3) < 0$, there is Coulomb repulsion between m_1 and m_3. $F_{BCF}(m_1, m_3)$ denotes the magnitude of the Coulomb repulsion, and m_1 and m_3 cannot be fused.

For a determined system, we can find in (13) that increasing BCF is associated with increased electrical charges and decreased square of the Coulomb evidence distance in the same recognition frame.

D. THE BASIC PROPERTIES OF THE PROPOSED BELIEF COULOMB FORCE FORMULA

Assumption 3: Assume that m_1 and m_2 are defined the same recognition framework Θ. In a determined system, Q_{m1} and Q_{m2} are the electrical charges of m_1 and m_2, $d(m_1, m_2)$ is the Coulomb evidence distance between the evidence, F_{BCF} is the Coulomb force between m_1 and m_2, and K_{ET} means the variable of evidence Coulomb force. The properties of the BCF formula can be identified as follows.

Nonnegative

Proof: First, according to Section 3.2, $d(m_1, m_2) > 0$, obviously $d^2 > 0$. Then, according to (13), $K_{ET} > 0$ can be known. When $d(m_1, m_2) > 0$, according to (10), Q_{m1} and $Q_{m1} > 0$. finally, Based on (12), the non-negativity of F_{BCF} can be obtained.

Symmetry

Proof: First, since m_1 and m_2 are in the same recognition frame according to Definition 9, so the Coulomb coefficient K_{ET} is determined. According to the symmetry of the Coulomb evidence distance (see section 3.2), there is $d(m_1, m_2) = d(m_2, m_1)$. It can be seen from (10) that the product of Q_{m1} and Q_{m2} is equal to Q_{m2} and Q_{m1}. Therefore, based on (12), we can get the symmetry of F_{BCF}, that is, $F_{BCF}(m_1, m_2) = F_{BCF}(m_2, m_1)$.

TABLE 1. The preliminary evidence obtained from sensors.

Time	Sensor	$m(\{A_1\})$	$m(\{A_2\})$	$m(\{A_3\})$
T=0s	S_1:$m_1(\cdot)$	0.99	0.01	0
T=0s	S_2:$m_2(\cdot)$	0.94	0.06	0
T=0s	S_3:$m_3(\cdot)$	0	0.01	0.99
T=5s	S_4:$m_4(\cdot)$	0.95	0.05	0
T=10s	S_5:$m_5(\cdot)$	0.97	0.03	0

IV. THE ESSENCE OF INFORMATION FUSION

Example 4: In the recognition frame $\Theta = \{A_1, A_2, A_3\}$, when T=0s, sensor 1, sensor 2 and sensor 3 obtain evidences m_1, m_2, m_3 respectively. Sensor 4 captures evidence m_4 in T=5s and sensor 5 gets evidence m_5 in T=10s. In Table 1, their BPA is calculated.

The evidence m_3 represents the conflict evidence, which does not support the proposition A_1 whereas other pieces of evidence do. According to the described BCF, the fusion process of the five distinct pieces of evidence is plotted in Fig. 2.

As 5 pieces of evidence of free state were displayed in Fig. 2(a), when T = 10, all the information has been collected. In detail, they are dispersed without correlation, and fusion is the simple combination of the evidence. Regardless, the result is not prone to determine the final decision due to the existence of disturbance m_3. whereas the evidence would be possible to gradually merge at each stage of obtaining evidence in the BCF system.

The three pieces of evidence obtained in stage 1 (T = 0) are shown in Fig. 2(b). Considering that under the BCF framework, $\rho(m_1, m_3) < 0$ means that there is Coulomb repulsion between m_1 and m_3 and they cannot be fused. The same is true for m_2 and m_3. Therefore, m_3 is high conflict evidence. Since $\rho(m_1, m_2) > 0$, there is Coulomb gravitational force between m_1 and m_2, which results in forming a new evidence M' from m_1 and m_2. The reliability of the proposition is higher than that of the initial pieces of evidence. At this time, as shown in Fig. 2(c), $\rho(m_3, M') < 0$ means that the Coulomb repulsion between m_3 and M' prevents them from fusing.

In stage 2 (T = 5s), when evidence m_4 is added, the status of each evidence in the system of BCF can be found in Fig. 2(d). Both $\rho(M', m_3)$ and $\rho(m_4, m_3)$ are less than 0, so m_3 is still the conflicting evidence. Since $\rho(M', m_4) > 0$, m_4 and M' are fused into a new evidence M'' as shown in Fig. 2(e). for the next stage, Fig. 2(f) displays the situation when adding evidence m_5. Fig. 2(g) plots the fusion results of the evidence in the system of BCF.

V. EXPERIMENTAL SIMULATION

Example 5.1 Suppose the recognition frame Θ has 20 elements, such as $\Theta = \{1,2,3, \cdots, 20\}$. Hence, the BPA of two different pieces of evidences m_1 and m_2 can be identified as follows

$m_1 : m_1(2,3,4)=0.05, m_1(7)=0.05, m_1(\Theta) = 0.1, m_1(A)=0.8,$
$m_2 : m_2(1,2,3,4,5)=1.$

Assuming that A is not a constant set, the 20 different conditions would vary with the number of the elements in A.

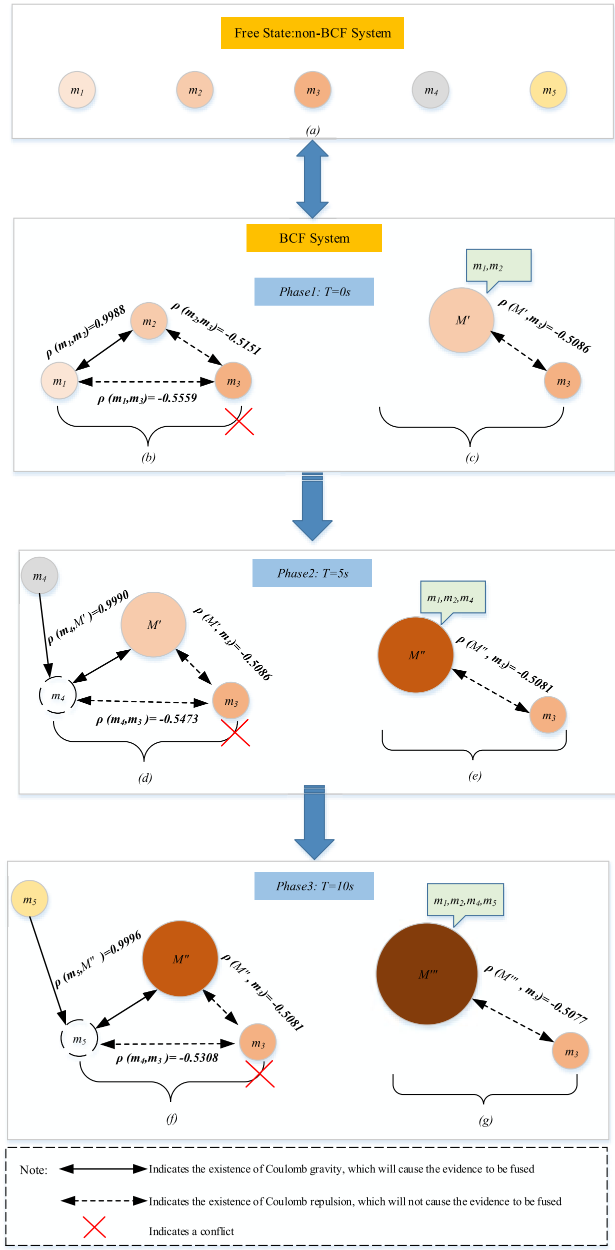

FIGURE 2. Information fusion modelling of five different pieces of evidence based on BCF.

Then the parameters, such as the electrical charges of m_1 and m_2, the square distance of the Coulomb evidence, and the value of BCF(F_{BCF}), are recorded in Table 2.

As displayed in Table 2, when the magnitude of A increases, the electrical charge Q_{m1} of m_1 would gradually increase whereas Q_{m2} remains constant. Fig. 3 and 4 show the two parameters d^2 and F_{BCF} varying with the size of A respectively.

Fig. 3 and 4 show that d_2 and F_{BCF} have opposite trends to the size of A respectively. In Fig. 3, when A is equal to the set $\{1,2,3,4,5\}$, d^2 becomes the minimum value. On the contrary, the farther A deviates from $\{1,2,3,4,5\}$, the larger d^2 is. As can

TABLE 2. The values of the parameters in the BCF formula.

A	K_{ET}	Q_{m1}	Q_{m2}	d^2	F_{BCF}
{1}	2^{-5}	3.0180	4.6657	0.7348	0.5976
{1,2}	2^{-5}	4.2283	4.6657	0.5483	1.1219
{1,2,3}	2^{-5}	5.1485	4.6657	0.3690	2.0292
{1,2,3,4}	2^{-5}	5.9704	4.6657	0.1964	4.4199
{1,2,3,4,5}	2^{-5}	6.7506	4.6657	0.0094	104.445
{1,2, …,6}	2^{-5}	7.5113	4.6657	0.1639	6.6819
{1,2,…,7}	2^{-5}	8.2627	4.6657	0.2808	4.2899
{1,2, …,8}	2^{-5}	9.0096	4.6657	0.3637	3.6109
{1,2, …,9}	2^{-5}	9.7541	4.6657	0.4288	3.3166
{1,2, …,10}	2^{-5}	10.4975	4.6657	0.4770	3.1811
{1,2, …,11}	2^{-5}	11.2404	4.6657	0.5202	3.1265
{1,2, …,12}	2^{-5}	11.9830	4.6657	0.5565	3.1187
{1,2, …,13}	2^{-5}	12.7254	4.6657	0.5872	3.1405
{1,2, …,14}	2^{-5}	13.4678	4.6657	0.6137	3.1819
{1,2, …,15}	2^{-5}	14.2101	4.6657	0.6367	3.2373
{1,2, …,16}	2^{-5}	14.9524	4.6657	0.6569	3.3029
{1,2, …,17}	2^{-5}	15.6947	4.6657	0.6748	3.3760
{1,2, …,18}	2^{-5}	16.4370	4.6657	0.6907	3.4551
{1,2, …,19}	2^{-5}	17.1793	4.6657	0.7050	3.5387
{1,2, …,20}	2^{-5}	17.9216	4.6657	0.7178	3.6261

[a]In the whole simulation, the flexible parameter was set to 1/4.

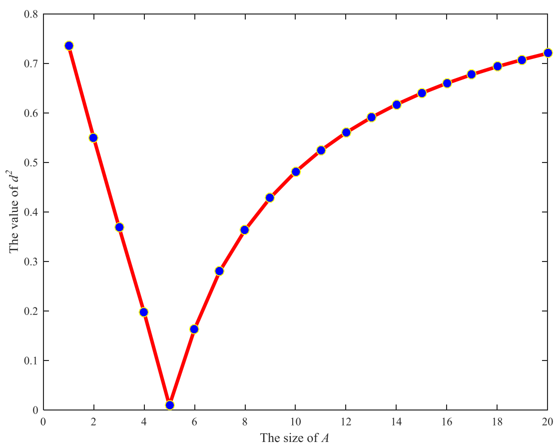

FIGURE 3. d^2 varies with the size of A.

be seen in Fig. 4, when A is close to *{1,2,3,4,5}*, the maximum F_{BCF} can be obtained. According to the physical meaning of BCF, when the Coulomb evidence distance d between m_1 and m_2 reaches the maximum value, the Coulomb force would be maximized. A larger size of A is thought to reflect the gradually increased Coulomb evidence distance between m_1 and m_2, and the less F_{BCF}.

Generally, the association between BCF and the relevant parameters is further revealed through the simulation. In a system of BCF, for a given recognition framework, with the Coulomb evidence distance d decreased, BCF becomes larger

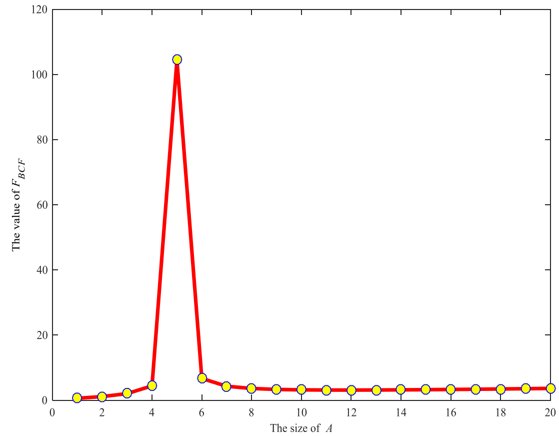

FIGURE 4. F_{BCF} varies with the size of A.

and the force between the evidence would increase. In a word, BCF is negatively proportional to the d^2.

VI. EVIDENCE CONFLICT MANAGEMENT BASED ON THE PROPOSED BELIEF COULOMB FORCE

Conflicts management in D-S evidence theory has been challenging the researchers for many years. Moreover, the correlation measurement among evidence is of great importance.

Dempster [1] firstly proposed the conflict coefficient k as the conflict degree between the evidence. Nevertheless, Liu [38] stated that k cannot represent the conflict effectively, and a *2-D* conflicting model was constructed within the pignistic probability distance and k as the reflection of the conflict. Afterward, a rule called ''(CWAC) rule'' was put forward by Lefèvre and Elouedi [46], where the distance measurement was based upon belief function according to Jousselme distance d [48], and an adaptive weighting was presented against Dempster rules and joint rules. Ma and Jiyao [47] performed a combination of conflict evidence and probability difference measurement. In Deng and Jiang [12], the correlation between 2 BPAs was investigated and applied in conflict evaluation. Then, in order to further explore the correlation, Jiang [44] introduced a new coefficient, as the measurement on the correlation between two pieces of evidence, with the consideration of both the non-intersection and the difference among the focal elements. Inspired by Jiang's method [44], Xiao *et al.* [50] proposed a new evidence correlation coefficient to model the belief function in evidence theory to support decision-making in uncertain environments.

Here, we compare the conflict degree between 2 groups BPA with the aforementioned approaches in example 5.1 and the result is summarized in Table 3 and Fig. 5.

According to Fig. 5, we can observe that the trends of the parameters d, k_r, and K_{ECC} are the same. When A is equal to the set {1,2,3,4,5}, the evidence conflict reaches the maximum value. On the contrary, the farther A deviates from {1,2,3,4,5}, the smaller the conflict value is. When the size of A is less than 5, DisSim is non-monotonic and cannot

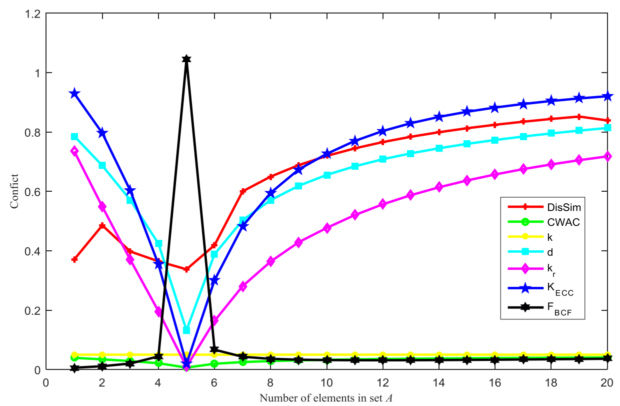

FIGURE 5. Comparison of conflicts between different parameter values.

TABLE 3. Comparisons of conflict degree.

A	k	d	$CWAC$	$DisSim$	k_r	K_{ECC}	F_{BCF}
1	0.05	0.7858	0.0393	0.3710	0.7348	0.9297	0.0060
1,2	0.05	0.6866	0.0343	0.4855	0.5483	0.7960	0.0112
1,2,3	0.05	0.5705	0.0285	0.3974	0.3690	0.6018	0.0203
1,2,3,4	0.05	0.4237	0.0212	0.3644	0.1964	0.3542	0.0442
1,2,3,4,5	0.05	0.1323	0.0066	0.3375	0.0094	0.0187	1.0444
1,2,…,6	0.05	0.3884	0.0195	0.4188	0.1639	0.3009	0.0668
1,2,…,7	0.05	0.5029	0.0251	0.6000	0.2808	0.4828	0.0429
1,2,…,8	0.05	0.5705	0.0285	0.6497	0.3637	0.5951	0.0361
1,2,…,9	0.05	0.6187	0.0309	0.6884	0.4288	0.6737	0.0332
1,2,…,10	0.05	0.6554	0.0328	0.7194	0.4770	0.7265	0.0318
1,2,…,11	0.05	0.6844	0.0342	0.7448	0.5202	0.7698	0.0313
1,2,…,12	0.05	0.7082	0.0354	0.7660	0.5565	0.8033	0.0312
1,2,…,13	0.05	0.7281	0.0364	0.7839	0.5872	0.8296	0.0314
1,2,…,14	0.05	0.7451	0.0372	0.7992	0.6137	0.8508	0.0318
1,2,…,15	0.05	0.7599	0.0380	0.8126	0.6367	0.8680	0.0324
1,2,…,16	0.05	0.7730	0.0386	0.8242	0.6569	0.8823	0.0330
1,2,…,17	0.05	0.7846	0.0392	0.8345	0.6748	0.8942	0.0338
1,2,…,18	0.05	0.7951	0.0397	0.8438	0.6907	0.9043	0.0346
1,2,…,19	0.05	0.8046	0.0402	0.8519	0.7050	0.9130	0.0354
1,2,…,20	0.05	0.8133	0.0407	0.8389	0.7178	0.9204	0.0363

[a]In this system the flexible variable is set to 1/4.
[b]In this study, every BCF is evenly divided into the same proportion (i.e., each BCF is divided by 100) without affecting the BCF properties as for the comparison facilitation.

effectively evaluate conflicting. CWAC remains at a low value and is not sensitive to the conflicting variation. Since the conflicting coefficient k always keeps at 0.5, it cannot be used as the identification of the varying evidence. Basically, with the increment of the size of A, F_{BCF} displayed the opposite trend compared with the other approach. Fewer conflicts between the evidence are thought to represent the larger Coulomb force.

In this example, although d and k_r can indicate the conflict variation, the result shows that the proposed BCF can better interpret the distinction of the conflict evidence according to physical theory. The trend can be vividly depicted in Fig. 5. Meanwhile, the potential on conflict measurement of BCF is revealed and promising for broad application.

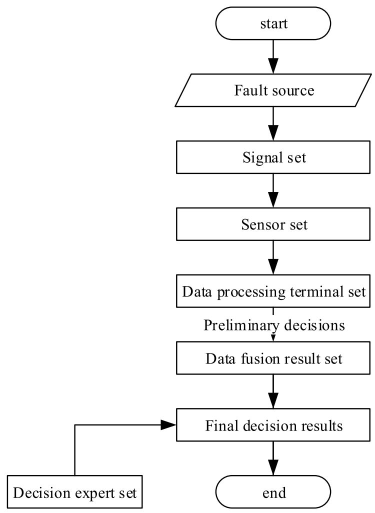

FIGURE 6. Machine fault diagnosis flowchart.

TABLE 4. The output of the multi-sensors.

m_i	A_1	A_2	A_3	A_4	Θ
m_1	0.06	0.68	0.02	0.04	0.20
m_2	0.02	0	0.79	0.005	0.14
m_3	0.02	0.58	0.16	0.04	0.20

VII. APPLICATION IN FAULT DIAGNOSIS

Integrating multiple sources of evidence to provide robust and effective malfunction diagnosis in industrial production is a perpetual challenge for the researchers. To prove the superiority of this approach, we applied BCF to actual fault diagnosis which is presented by Jiang *et al.* [9]. The whole process of malfunction diagnosis is plotted in Fig. 6.

A. APPLICATION BACKGROUND

The characteristic information such as acceleration m_1, velocity m_2, displacement m_3, and so on, is collected from three sensors and converted to BPA and shown in Table 4, where A_1, A_2, A_3, and A_4 stand for four states of the rotor: normal operation, unbalanced, out of adjustment, and loose base. Thus establishing a recognition framework, namely $\Theta = \{A_1, A_2, A_3, A_4\}$.

According to the collected data, it should be noted that the information m_2 conflicts with others since it does not support A_2, whereas m_1 and m_3 highly support A_2.

B. BCF-BASED FAULT DIAGNOSIS

To fuse the data recorded from 3 sensors, we adopted Deng method [35]. However, the evidence information recorded from the sensor is represented by similarity derived from BCF rather than the evidence distance [48]. The method is briefly described as follows.

Step 1: A BCF matrix (BCFM) is constructed as the reflection of the correlation between two pieces of evidence. Assuming there are n pieces of evidence, BCFM can be defined in (15), as shown at the bottom of the next page,

TABLE 5. The averaged evidence.

$m(A_1)$	$m(A_2)$	$m(A_3)$	$m(A_4)$	$m(\Theta)$
0.04	0.6296	0.0905	0.04	0.2

where $F_{BCF}(m_i, m_j)$ stands for the Coulomb force between the evidence m_i and m_j, $i=1, 2\ldots n$, $j=1, 2..n$, and $i \neq j$. The value of ξ is not defined.

Step 2: Describe the similarities between the evidence. Expressed as follows

$$F_{BPA}(m_i, m_j) = \frac{F_{BCF}(m_i, m_j)}{(1-\rho(m_i, m_j))}, \tag{16}$$

where $F_{BPA}(m_i, m_j)$ and $\rho(m_i, m_j)$ [45] denote the similarity and Pearson correlation coefficient between m_i and m_j, $i=1, 2\ldots n$, $j=1, 2..n$, and $i \neq j$. If $\rho(m_i, m_j) > 0$, there is Coulomb gravitational force between m_i, *and* m_j. The larger the ρ is, the smoother the fusion between m_i and m_j would be. If $\rho(m_i, m_j) < 0$, there is Coulomb repulsion between the evidence. The smaller the $\rho(m_i, m_j)$ is, the more difficultly it is to merge for m_i and m_j.

Step 3: Calculate the credibility of the evidence. The expression of the trust degree of the evidence subject is shown below

$$su\left(m_i\right) = \sum\nolimits_{j=1, j\neq i}^{n} F_{BPA}\left(m_i, m_j\right). \tag{17}$$

Among them, $F_{BPA}(m_i, m_j)$ stands for the degree of support between m_i and m_j, and $su(m_i)$ represents the degree of support for m_i.

Crd_i is the credibility of the evidence m_i, which is defined as

$$Crd_i = \frac{su\left(m_i\right)}{\sum_{i=1}^{n} su\left(m_i\right)}. \tag{18}$$

Step 4: find the average weight of all evidence, as shown in

$$AVE\left(m\right) = \sum\nolimits_{i=1}^{n} (Crd_i \times m_i). \tag{19}$$

Step 5: Use Demoster's combination rule (4) to perform $n-1$ fusions to obtain the final fusion evidence, and select the most extensive hypothesis under the information fusion as the recognition result.

Generally, in the specific calculation process, the credibility of three groups of evidence are $\mathrm{Crd}_1 = 0.4995$, $\mathrm{Crd}_2 = 0.0.0007$, and $\mathrm{Crd}_3 = 0.4998$, which are obtained by using (18). The average weight of the evidence is received by (19), see Table 5.

TABLE 6. The final outputs of Dempster's combination rule.

$m(A_1)$	$m(A_2)$	$m(A_3)$	$m(A_4)$	$m(\Theta)$
0.0097	0.9397	0.0276	0.0097	0.0133

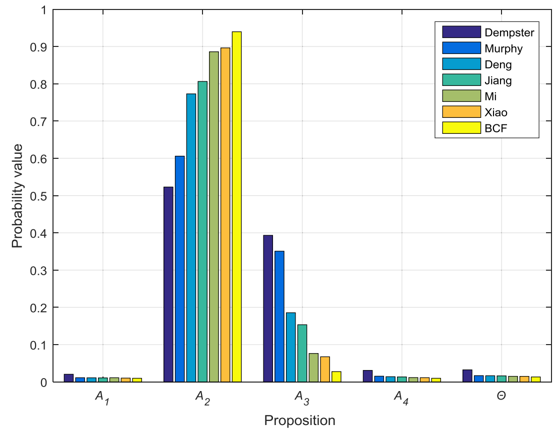

FIGURE 7. The probability comparison among the existing techniques.

TABLE 7. The original output of sensors and diagnosis results.

Sensor type	A_1	A_2	A_3	A_4	Θ	Diagnosis result
Acceleration	0.06	0.68	0.02	0.04	0.20	Uncertainty
Velocity	0.02	0	0.79	0.005	0.14	Uncertainty
Displacement	0.02	0.58	0.16	0.04	0.20	Uncertainty

TABLE 8. Comparisons of some existing techniques.

Method	A_1	A_2	A_3	A_4	Θ	Diagnosis result
Dempster	0.0205	0.5230	0.3933	0.0309	0.0324	Uncertainty
Murphy	0.0112	0.6059	0.3508	0.0153	0.0168	Uncertainty
Deng	0.0110	0.7730	0.1856	0.0139	0.0165	Uncertainty
Jiang	0.0108	0.8063	0.1534	0.0134	0.0162	Unbalance
Mi	0.0111	0.8860	0.0763	0.0116	0.0149	Unbalance
Xiao	0.0102	0.8964	0.0674	0.0113	0.0148	Unbalance
BCF	0.0097	0.9397	0.0276	0.0097	0.0133	Unbalance

Thus, the fusion is regulated with Dempster's combination rules, and the final results can be seen in Table 6.

C. ANALYSIS AND DISCUSSION

The result of the fault diagnosis can be reflected by the probability of supporting the malfunction. In this article, the threshold is set to 0.8 after several simulations. Table 7 shows the initial diagnosis results and the fault diagnosis results after the fusion are displayed in Table 8 and Fig. 7.

Basing upon the comparison of fault diagnosis results in Table 7 and Table 8, the advantages of multi-source sensor data fusion are obvious. More specifically, in Table 7, it is

$$\begin{bmatrix} \xi & F_{BCF}\left(m_1, m_2\right) & \cdots & F_{BCF}\left(m_1, m_j\right) & \cdots & F_{BCF}\left(m_1, m_n\right) \\ \vdots & \vdots & \vdots & \vdots & \vdots & \vdots \\ F_{BCF}\left(m_i, m_1\right) & F_{BCF}\left(m_i, m_2\right) & \cdots & F_{BCF}\left(m_i, m_j\right) & \cdots & F_{BCF}\left(m_i, m_n\right) \\ \vdots & \vdots & \vdots & \vdots & \vdots & \vdots \\ F_{BCF}\left(m_n, m_1\right) & F_{BCF}\left(m_n, m_2\right) & \cdots & F_{BCF}\left(m_n, m_j\right) & \cdots & \xi \end{bmatrix}, \tag{15}$$

not prone to make a correct judgment if we only regard one feature as the reflection of the machine's working state. Under the threshold of 0.8, this evidence indicates that they give an indeterminate answer before the combination of evidence. Through Fig. 7 and Table 8, we can find out that once Dempster [1], Murphy [34], and Yong *et al.* [35] are utilized to fuse the obtained evidence, it is not superb enough for us to make a decision, because their $m(A_2)$ are 0.523, 0.6059, and 0.7730, respectively, and smaller than the threshold of 0.8. The approach presented by Jiang [44], Mi and Kang [49], and Xiao *et al.* [50] can only identify that the equipment failure is unbalanced, as they obtain the values of $m(A_2)$ are 0.8063, 0.886, and 0.8964, respectively, whereas the value of $m(A_2)$ obtained by the proposed method reaches 0.9397, which seems to make a more robust and accurate judgment.

In summary, this example verifies the effectiveness and robustness of BCF in conflict situations, and promises future application.

VIII. CONCLUSION AND DISCUSSION

A new concept of BCF was introduced into D-S evidence theory in this study. The work can be summarized as follows. First, as far as we concerned, this is the first time when Coulomb law is introduced into evidence theory from natural science. Second, the BCF formula is utilized as the measurement of Coulomb force between the evidence. By modeling the evidence fusion, the rationale of BCF in the fusion process has been clearly elaborated and the problem of under what conditions can fuse the evidence has been solved. Finally, the resolution on conflict management in D-S evidence theory and the application in fault diagnosis, which demonstrate the effectiveness and superiority.

However, several limitations in BCF still remained to be overcome. For instance, as a measurement of the amount of information in evidence, is there an alternative suitable information entropy? How to improve the reliability of BCF and apply it to more realistic issues? Hence, we would consider the vector nature of Coulomb force and lay the foundation of a completed BCF theory. On the other hand, BCF would be performed to deal with the anti-monitoring of transmission media, interference interception, and measurement.

REFERENCES

[1] A. P. Dempster, "Upper and lower probabilities induced by a multivalued mapping," *Ann. Math. Statist.*, vol. 38, no. 2, pp. 325–339, Apr. 1967.
[2] G. Shafer, "Dempster–Shafer theory," in *Encyclopedia of Artificial Intelligence*. Jan. 1992, pp. 330–331.
[3] A. Ratnaparkhi, "Learning to parse natural language with maximum entropy models," *Mach. Learn.*, vol. 34, nos. 1–3, pp. 151–175, 1999.
[4] F. Xiao and W. Ding, "Divergence measure of pythagorean fuzzy sets and its application in medical diagnosis," *Appl. Soft Comput.*, vol. 79, pp. 254–267, Jun. 2019.
[5] L. A. Zadeh, "Fuzzy sets, information and control," *Inf. Control*, vol. 8, no. 3, pp. 338–353, 1965.
[6] I. Dzitac, F. G. Filip, and M.-J. Manolescu, "Fuzzy logic is not fuzzy: World-renowned computer scientist Lotfi A. Zadeh," *Int. J. Comput. Commun. Control*, vol. 12, no. 6, p. 748, Dec. 2017.
[7] Q. Liu, Y. Tian, and B. Kang, "Derive knowledge of Z-number from the perspective of Dempster–Shafer evidence theory," *Eng. Appl. Artif. Intell.*, vol. 85, pp. 754–764, Oct. 2019.
[8] Y. Tian and B. Kang, "A modified method of generating Z-number based on OWA weights and maximum entropy," *Soft Comput.*, vol. 24, no. 20, pp. 15841–15852, Oct. 2020.
[9] W. Jiang, B. Wei, C. Xie, and D. Zhou, "An evidential sensor fusion method in fault diagnosis," *Adv. Mech. Eng.*, vol. 8, no. 3, Mar. 2016, Art. no. 168781401664182.
[10] J. P. Walsh, "Selectivity and selective perception: An investigation of managers' belief structures and information processing," *Acad. Manage. J.*, vol. 31, no. 4, pp. 873–896, Dec. 1988.
[11] X. Deng and W. Jiang, "D number theory based game-theoretic framework in adversarial decision making under a fuzzy environment," *Int. J. Approx. Reasoning*, vol. 106, pp. 194–213, Mar. 2019.
[12] X. Deng and W. Jiang, "Evaluating green supply chain management practices under fuzzy environment: A novel method based on d number theory," *Int. J. Fuzzy Syst.*, vol. 21, no. 5, pp. 1389–1402, Jul. 2019.
[13] Y. Tian, L. Liu, X. Mi, and B. Kang, "ZSLF: A new soft likelihood function based on Z-numbers and its application in expert decision system," *IEEE Trans. Fuzzy Syst.*, early access, May 25, 2020, doi: 10.1109/TFUZZ.2020.2997328.
[14] M. Jing and Y. Tang, "A new base basic probability assignment approach for conflict data fusion in the evidence theory," *Appl. Intell.*, vol. 51, no. 2, pp. 1–13, 2021.
[15] Y. Tang, D. Wu, and Z. Liu, "A new approach for generation of generalized basic probability assignment in the evidence theory," *Pattern Anal. Appl.*, vol. 1, no. 6, pp. 1–17, Apr. 2020.
[16] F. Liu, X. Gao, J. Zhao, and Y. Deng, "Generalized belief entropy and its application in identifying conflict evidence," *IEEE Access*, vol. 7, pp. 126625–126633, 2019.
[17] L. Pan and Y. Deng, "Probability transform based on the ordered weighted averaging and entropy difference," *Int. J. Comput. Commun. Control*, vol. 15, no. 4, p. 3743, 2020.
[18] K. Xie and F. Xiao, "Negation of belief function based on the total uncertainty measure," *Entropy*, vol. 21, no. 1, p. 73, Jan. 2019.
[19] L. Fei, J. Xia, Y. Feng, and L. Liu, "A novel method to determine basic probability assignment in Dempster–Shafer theory and its application in multi-sensor information fusion," *Int. J. Distrib. Sensor Netw.*, vol. 15, no. 7, Jul. 2019, Art. no. 155014771986587.
[20] V. Venkatesh, P. Raj, K. Kannan, and P. Balakrishnan, "Precision centric framework for activity recognition using dempster Shaffer theory and information fusion algorithm in smart environment," *J. Intell. Fuzzy Syst.*, vol. 36, no. 3, pp. 2117–2124, Mar. 2019.
[21] W. Liu, T. Wang, T. Zang, Z. Huang, J. Wang, T. Huang, X. Wei, and C. Li, "A fault diagnosis method for power transmission networks based on spiking neural P systems with self-updating rules considering biological apoptosis mechanism," *Complexity*, vol. 2020, pp. 1–18, Jan. 2020.
[22] Q. Gao and D.-L. Xu, "An empirical study on the application of the evidential reasoning rule to decision making in financial investment," *Knowl.-Based Syst.*, vol. 164, pp. 226–234, Jan. 2019.
[23] M. Li, H. Xu, and Y. Deng, "Evidential decision tree based on belief entropy," *Entropy*, vol. 21, no. 9, p. 897, Sep. 2019.
[24] L. A. Zadeh, "A simple view of the Dempster–Shafer theory of evidence and its implication for the rule of combination," *Adv. Fuzzy Syst.-Appl. Theory*, vol. 7, no. 2, pp. 674–679, 1996.
[25] E. Lefevre, O. Colot, and P. Vannoorenberghe, "Belief function combination and conflict management," *Inf. Fusion*, vol. 3, no. 2, pp. 149–162, Jun. 2002.
[26] R. R. Yager, "On the Dempster–Shafer framework and new combination rules," *Inf. Sci.*, vol. 41, no. 2, pp. 93–137, Mar. 1987.
[27] R. R. Yager, "Quasi-associative operations in the combination of evidence," *Kybernetes*, vol. 16, no. 1, pp. 37–41, 1987.
[28] T. Inagaki, "Interdependence between safety-control policy and multiple-sensor schemes via Dempster–Shafer theory," *IEEE Trans. Rel.*, vol. 40, no. 2, pp. 182–188, Jun. 1991.
[29] D. Fixsen and R. P. S. Mahler, "The modified Dempster–Shafer approach to classification," *IEEE Trans. Syst., Man, Cybern. A, Syst. Humans*, vol. 27, no. 1, pp. 96–104, Jan. 1997.
[30] M. Daniel, "Associativity in combination of belief functions; a derivation of minC combination," *Soft Comput. Fusion Found., Methodol. Appl.*, vol. 7, no. 5, pp. 288–296, Apr. 2003.
[31] F. Xiao, "Generalization of Dempster–Shafer theory: A complex mass function," *Int. J. Speech Technol.*, vol. 50, no. 10, pp. 3266–3275, Oct. 2020.

[32] W. Ma, Y. Jiang, and X. Luo, "A flexible rule for evidential combination in Dempster–Shafer theory of evidence," *Appl. Soft Comput.*, vol. 85, Dec. 2019, Art. no. 105512.
[33] R. Haenni, "Comments on about the belief function combination and the conflict management problem," *Inf. Fusion*, vol. 3, no. 4, pp. 237–239, 2002.
[34] C. K. Murphy, "Combining belief functions when evidence conflicts," *Decis. Support Syst.*, vol. 29, no. 1, pp. 1–9, Jul. 2000.
[35] D. Yong, S. WenKang, Z. ZhenFu, and L. Qi, "Combining belief functions based on distance of evidence," *Decis. Support Syst.*, vol. 38, no. 3, pp. 489–493, Dec. 2004.
[36] F. Xiao, "A new divergence measure for belief functions in D–S evidence theory for multisensor data fusion," *Inf. Sci.*, vol. 514, pp. 462–483, Apr. 2020, doi: 10.1016/j.ins.2019.11.022.
[37] F. Xiao, "Multi-sensor data fusion based on the belief divergence measure of evidences and the belief entropy," *Inf. Fusion*, vol. 46, pp. 23–32, Mar. 2019.
[38] W. Liu, "Analyzing the degree of conflict among belief functions," *Artif. Intell.*, vol. 170, no. 11, pp. 909–924, Aug. 2006.
[39] K. Lee and K. Park, "Modeling eddy currents with boundary conditions by using Coulomb's law and the method of images," *IEEE Trans. Magn.*, vol. 38, no. 2, pp. 1333–1340, Mar. 2002.
[40] S. Jiang, C. Zhang, W. Wu, and S. Chen, "Combined economic and emission dispatch problem of wind-thermal power system using gravitational particle swarm optimization algorithm," *Math. Problems Eng.*, vol. 2019, pp. 1–19, Nov. 2019.
[41] A. A. Nagra, F. Han, Q.-H. Ling, and S. Mehta, "An improved hybrid method combining gravitational search algorithm with dynamic multi swarm particle swarm optimization," *IEEE Access*, vol. 7, pp. 50388–50399, 2019.
[42] Y. Deng, "Deng entropy," *Chaos, Solitons Fractals*, vol. 91, pp. 549–553, Oct. 2016.
[43] D. Zhou, Y. Tang, and W. Jiang, "A modified belief entropy in Dempster–Shafer framework," *PLoS ONE*, vol. 12, no. 5, May 2017, Art. no. e0176832.
[44] W. Jiang, "A correlation coefficient for belief functions," *Int. J. Approx. Reasoning*, vol. 103, pp. 94–106, Dec. 2018.
[45] Y. Liu, Y. Mu, K. Chen, Y. Li, and J. Guo, "Daily activity feature selection in smart homes based on pearson correlation coefficient," *Neural Process. Lett.*, vol. 51, no. 2, pp. 1771–1787, Apr. 2020.
[46] E. Lefévre and Z. Elouedi, "How to preserve the conflict as an alarm in the combination of belief functions?" *Decis. Support Syst.*, vol. 56, pp. 326–333, Dec. 2013.
[47] M. Ma and J. An, "Combination of evidence with different weighting factors: A novel probabilistic-based dissimilarity measure approach," *J. Sensors*, vol. 2015, Mar. 2015, Art. no. 509385.
[48] A.-L. Jousselme, D. Grenier, and É. Bossé, "A new distance between two bodies of evidence," *Inf. Fusion*, vol. 2, no. 2, pp. 91–101, Jun. 2001.
[49] X. Mi and B. Kang, "On the belief universal gravitation (BUG)," *Comput. Ind. Eng.*, vol. 148, Oct. 2020, Art. no. 106685.
[50] F. Xiao, Z. Cao, and A. Jolfaei, "A novel conflict measurement in decision-making and its application in fault diagnosis," *IEEE Trans. Fuzzy Syst.*, vol. 29, no. 1, pp. 186–197, Jan. 2021.

BO FU was born in Hubei, China. He is currently a Professor with the School of Electrical and Electronic Engineering, Hubei University of Technology. He has accomplished the projects "Research and Application of Online Active Preview, Analysis and Evaluation of Complex Fault Handling Strategies" from the China Electric Power Research Institute, and "Research on Key Technologies of UAV Inspection Scheme Based on Fast Charging of Super Capacitors" from Hubei Electric Power Company. He has published multiple articles, especially journals like An improved mixed integer linear programming based on symmetry diminishing for unit commitment of hybrid power system, which has been highly cited. His main research interest includes power systems and automation.

JINWEI FANG is currently pursuing the master's degree with the School of Electrical and Electronic Engineering, Hubei University of Technology, Wuhan, China. His current research interests include image processing, Dempster–Shafer evidence theory, and multi-source information fusion.

XILIN ZHAO was born in Hubei, China. He received the D.Sc. degree in system analysis and integration from the Huazhong University of Science and Technology, Wuhan, China, in 2009. He is currently a Professor with the Hubei University of Technology. His research interest includes electric engineering.

XING CHEN was born in Wuhan, Hubei, China, in 1993. He received the B.S. degree in electrical engineering from the Hubei University of Technology, in 2011, and the M.S. degree from the Illinois Institute of Technology, Chicago, IL, USA, in 2015. He is currently pursuing the Ph.D. degree in mechanical and electrical engineering with the University of Southern Queensland, QLD, Australia. His research interests include signal processing, and the development of anesthesia monitoring techniques.

KANG XU was born in Hubei, China. He is currently pursuing the degree in electrical engineering with the Hubei University of Technology. His research interests include Dempster–Shafer evidence theory, power system automation, and machine learning.

ZHANGQING HE received the Ph.D. degree from the School of Optics and Electronic Information, Huazhong University of Science and Technology. He is currently a Professor with the School of Electrical and Electronic Engineering, Hubei University of Technology. In recent years, he has been engaged in the research of integrated circuit hardware security, participated in multiple scientific research projects.